

# Internal Conversion in the Chromophore of the Green Fluorescent Protein: Temperature Dependence and Iviscosity Analysis

Konstantin L. Litvinenko, Naomi M. Webber, and Stephen R. Meech\*

School of Chemical Sciences and Pharmacy, University of East Anglia, Norwich NR4 7TJ, U.K.

Received: November 1, 2002; In Final Form: January 31, 2003

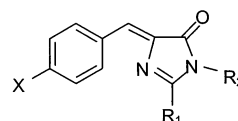
The temperature dependence of internal conversion in model compounds of the chromophore of the green fluorescent protein and one of its mutants has been measured. The strong temperature dependence persists in all charge forms of the model compounds, in all solvents and in a polymer matrix. The ultrafast internal conversion mechanism is thus an intrinsic property of the chromophore skeleton, rather than one of a specific charge or hydrogen-bonded form. An isoviscosity analysis shows that the coordinate which promotes internal conversion is essentially barrierless at room temperature. At reduced temperatures (or high viscosity) there is evidence for the formation of a small barrier. This may reflect a change in the nature of the microscopic solvent dynamics close to the glass transition temperature. In all cases the viscosity dependence of the rate constant for internal conversion is very weak, being approximately proportional to viscosity raised to the power of  $0.25 \pm 0.06$ . This suggests weak coupling between the relevant coordinate and macroscopic solvent viscosity. It is suggested that a potential candidate for the coordinate which promotes internal conversion is the volume-conserving “hula twist”.

## 1. Introduction

The green fluorescent protein (GFP) is very widely used as a genetically encoded noninvasive fluorescence marker in bioimaging.<sup>1,2</sup> The structure of GFP has been established, and the chromophore identified as a *p*-hydroxybenzylidene imidazolidinone, Chart 1, formed from a cyclization and oxidation reaction of three adjacent amino acids.<sup>3–5</sup> The quantum yield of fluorescence of the chromophore in the intact protein has been measured as  $\approx 0.8$ .<sup>1</sup> The fundamental photophysical processes of GFP have been established in both ultrafast fluorescence experiments and simulations. The key processes are facile excited-state proton transfer from the neutral excited chromophore to form the fluorescent anionic state, and an infrequent structural reorganization in the protein to accommodate the new anionic excited state.<sup>6,7</sup>

One intriguing observation, which is not yet explained, is that the denatured protein, isolated fragments of protein containing the chromophore, and synthetic model compounds of the chromophore, are all essentially nonfluorescent in fluid solution at room temperature.<sup>5,8</sup> Further, although many mutants of the protein have a high fluorescence quantum yield, Kummer et al. have shown that some mutants are only rather weakly fluorescent.<sup>9</sup> Clearly it is necessary to understand the mechanism of radiationless decay in the chromophore, to aid the interpretation and optimization of the photophysical properties of GFP mutants for bioimaging and other applications. There are additional reasons why an understanding of the mechanism of the dramatic suppression of radiationless decay by the GFP matrix is important. At a fundamental level, the  $10^4$  fold enhancement in fluorescence quantum yield when the protein structure is formed around the chromophore suggests a highly effective protein–pigment interaction. An understanding of this interaction may impact on a wider understanding of biochromatics. At a practical level, many theoretical calculations of the electronic structure

## CHART 1



**I** X = OH, R<sub>1</sub> = R<sub>2</sub> = CH<sub>3</sub>

**II** X = H, R<sub>1</sub> = CH<sub>3</sub>, R<sub>2</sub> = CO<sub>2</sub>C<sub>2</sub>H<sub>5</sub>

of GFP use as their starting-point structures similar to the model compounds **I** and **II**, rather than the actual structure in the protein.<sup>10–14</sup> A key test of the suitability of such theoretical models for protein calculations will be their ability to reproduce the observed chromophore dynamics in simpler systems.

We initiated a study of the radiationless relaxation of compounds **I** and **II** in solution. Using ultrafast polarization spectroscopy the dominant mechanism of ground-state recovery in **I** was identified as internal conversion (IC).<sup>15,16</sup> In a series of *n*-alcohols the IC rate was found to be only a very weak function of medium viscosity  $\eta$ , while the reorientation of the entire molecule was well described by a linear  $\eta$  dependence, as expected for diffusive reorientation.<sup>16,17</sup> In addition, the strong temperature dependence of the fluorescence yield was found to be rather insensitive to the solvent glass transition temperature.<sup>15</sup> It was proposed that these data are consistent with a mechanism for IC involving a coordinate which does not require the displacement of large volumes of solvent, but may be thermally activated over a low barrier. The data were not sufficient to distinguish between thermally activated or weakly friction-controlled mechanisms. The rate of IC was also found to depend somewhat on the charge state of **I**, with the fastest relaxation being for the neutral, and longest for the anion.<sup>17</sup>

More recently ultrafast fluorescence spectroscopy has been used to investigate radiationless relaxation in **I**.<sup>18,19</sup> Femtosecond fluorescence up-conversion measurements revealed a fluorescence decay for **I**<sup>–</sup> in *n*-alcohols at 294 K, which is well described by a sum of two exponential terms: a subpicosecond

\* Corresponding author. E-mail: s.meech@uea.ac.uk.

component, independent of  $\eta$ , and a picosecond component that had a weak  $\eta$  dependence.<sup>18</sup> Kummer et al. used a streak camera to record the fluorescence decay of compounds similar to **I** and **I**<sup>-</sup> over a very wide viscosity range.<sup>19</sup> They reported a stronger viscosity dependence of  $\eta^{0.5}$  than that in ref 18. We will return to the viscosity dependence below. Other groups have investigated the spectroscopy of compounds similar to **I** as models for GFP spectroscopy.<sup>20–22</sup> In particular Schellenberg and co-workers have demonstrated that there are significant differences in the Raman spectra of **I** and GFP, while **I** has a low-temperature photochemical hole-burning behavior which is rather similar to that observed in GFP.<sup>21,22</sup>

The time-resolved measurements<sup>15–19</sup> cannot reveal the identity of the coordinate which couples ground and excited states to facilitate IC. Consideration of the known photophysical properties of a number of compounds structurally related to **I**, such as cyanine and stilbene dyes, suggest that rotation about one or both of the bridging carbon–carbon bonds is a strong candidate.<sup>23,24</sup> This possibility has been further investigated through quantum chemical calculations on **I** (as far as we are aware there are no similar calculations on **II**) by two groups.<sup>10,25</sup> For rotation about the double bond, Voityuk et al. found energy minima for the planar ground state and the 90° twisted excited state. This suggests excited-state rotation about this bond as a possible coordinate promoting IC, as the rate of IC is critically, exponentially, dependent on the energy separation between initial and final states. The approach of excited and ground states was calculated to be very close in the cation, leading to the expectation of rapid IC, but less close in the neutral and anion forms.<sup>25</sup> For rotation about the single bond, the ground and excited states were calculated to approach only in the anion, but not the neutral or cation.

A related set of calculations was presented by Weber et al. for planar and 90° twisted forms of the neutral and anionic states of **I**.<sup>10</sup> The results were qualitatively similar to those of Voityuk et al. (though they were quantitatively different, indicating the uncertainties associated with this kind of calculation). Weber et al. also presented results for a concerted twist motion about both bridging bonds (the “hula twist”<sup>26,27</sup>) which showed close approach of ground and excited states for both anionic and neutral forms of **I** at a twist angle of 90°. This result is consistent with rapid IC in both **I** and **I**<sup>-</sup>, as observed experimentally.<sup>16,17</sup> In addition this mode displaces little solvent, and might not therefore be expected to be strongly sensitive to  $\eta$ , in agreement with experiments at low and moderate viscosity.<sup>15–17</sup>

In this paper the objective is to provide a more detailed insight into radiationless decay in **I**, and to investigate for the first time radiationless decay in **II**. Compound **II** is of particular interest as it is the model for a blue-emitting mutant of GFP (tyr66phe) in which dynamics associated with the phenolic hydroxyl substituent are blocked.<sup>8,28</sup> In the following the potentially intermingled effects of a thermal barrier in, and solvent friction effects upon, the coordinate leading to IC will be separated by an isoviscosity analysis.<sup>23</sup> To achieve this we will use both temperature-dependent steady-state fluorescence and ultrafast ground-state recovery measurements, in a range of solvents, including a polymer matrix. The small temperature (or viscosity) dependent barrier and the weak viscosity dependence of  $k_{IC}$  observed are discussed in terms of the likely candidate promoting IC, and its interaction with the environment.

## 2. Measurements and Analysis

The experimental apparatus for ultrafast measurements has been described in detail elsewhere.<sup>16</sup> The second harmonic of

an amplified titanium sapphire laser provides sub 200 fs pulses at 396 nm. These are used in the standard ultrafast polarization spectroscopy geometry, to record the ground-state recovery dynamics following  $S_0 \rightarrow S_1$  electronic excitation. Both population and orientational dynamics are measured in the polarization spectroscopy experiment.<sup>16,29,30</sup> The latter are observed in the case of **I** because of a minor radiationless relaxation channel to an unidentified bottleneck state.<sup>16</sup> The resulting ground-state recovery through orientational relaxation is well described by a hydrodynamic Stokes–Einstein–Debye model of rotational diffusion with near “stick” boundary conditions. This was established earlier for **I** and **I**<sup>-</sup>,<sup>16</sup> and was also found here for **I**<sup>+</sup> (data not shown).<sup>31</sup> Fortunately, the time scale for the IC and reorientation are quite distinct and so easily separated, and in the following we will concentrate exclusively on the population dynamics.

Ultrafast polarization spectroscopy experiments could only be conducted on **I**, its anion and cation, as the absorbance of **II** is negligible at 396 nm; the solvent and pH dependence of the electronic spectra of **I** and **II** are discussed in more detail elsewhere.<sup>32</sup> In all ultrafast measurements the optical density of the solutions was adjusted to be approximately 1.0 in a 2 mm cuvette at 400 nm. Analysis of the transient data was as previously described,<sup>16</sup> and yields directly  $\langle \tau_{IC} \rangle = k_{IC}^{-1}$ , where the angle brackets indicate the weighted average of the bi-exponential fit to the ultrafast ground-state recovery.

Stationary-state fluorescence measurements were made in a 1 cm path length cuvette made from square tubing, contained in an Oxford Instruments cryostat (DN 1704). This was placed in the sample cavity of a Spex Fluoramax 2 spectrofluorimeter. The cuvette space in the DN 1704 was filled with dry nitrogen gas as a heat exchanger. Sample concentrations were adjusted to give an optical density of ca. 0.1 at the excitation wavelength, which was chosen to be 20 nm to the short wavelength side of the absorption maximum, so as to minimize contributions from solvent Raman scattering to the signal.<sup>31</sup> Measurements were made at temperatures down to 77 K, the samples being equilibrated at each temperature until no further change in fluorescence intensity was observed.

The radiationless decay rate  $k_{IC}$  was calculated from the measured fluorescence spectra according to:

$$\langle k_{IC} \rangle = k_f \left( \frac{1 - \Phi_F^R}{\Phi_F^R} \right) \quad (1)$$

where  $k_f$  is the radiative rate constant and  $\Phi_F^R$  is the fluorescence quantum yield relative to that at 77 K,  $\Phi_F^R = (\Phi_F/\Phi_F^{77})$ . Since the spectral profile is essentially independent of temperature (see below), the  $\Phi_F^R$  measurements were taken from intensity ratios, rather than the integrated area, to avoid the need for subtraction of the solvent Raman contribution, which was significant at temperatures above 200 K. To calculate  $k_{IC}$  a value for  $k_f$  is required. As this is unknown for **I** and **II**, a value of  $2.5 \times 10^8 \text{ s}^{-1}$  has been assumed for all solutes in all solvents at every temperature. This value is based on the measured quantum yield and known nanosecond lifetime of wild-type GFP.<sup>33</sup> The value assumed is justified on the grounds that **I** has a similar oscillator strengths to GFP. The assumption of a temperature and solvent independent value of  $k_f$  is based on the observation that the electronic spectra of **I** are only weakly dependent on these variables.<sup>31,32</sup>

Once a value for  $k_{IC}$  is determined its dependence on viscosity and temperature can be analyzed. As discussed in the Introduction, the rate of IC is in general a function of both the friction

$\zeta$  experienced by the coordinate coupling the ground and excited states and the height of any potential barrier  $E$  along that coordinate:<sup>23,24</sup>

$$k_{\text{IC}} = F(\zeta)\exp(-E/RT) \quad (2)$$

Since both exponential and preexponential are functions of temperature, an Arrhenius analysis leads only to an apparent activation energy, and it is desirable to have some means of separating the two functions. A straightforward approach is to first model the friction experienced by the coordinate promoting IC (inherently a microscopic friction) by a macroscopic parameter, the medium viscosity. If this hydrodynamic approximation (which is very successful in measurements of rotational diffusion)<sup>34,35</sup> is accepted, then it is possible to measure  $k_{\text{IC}}$  in a series of similar solvents at temperatures chosen such that in each case the macroscopic viscosity is the same. In that case an “isoviscosity” plot of  $\ln k_{\text{IC}}$  against  $1/T$  will yield the isoviscosity activation energy, which can then be factored out of all subsequent measurements, to yield separately the friction dependence. Such a series of measurements is described below for **I** and **II**.

The form of  $F(\zeta)$  so recovered can be quite informative with regard to the dynamics of the IC reaction. In the case of an appreciable barrier in the isomerization coordinate  $F(\zeta)$  can be represented by Kramers' expression,<sup>36</sup> which, in the limit of a small curvature of the barrier and/or a high viscosity (the Smoluchowski limit), predicts a linear dependence of  $k_{\text{IC}}$  on  $\eta^{-1}$ .<sup>37</sup> A second important limit is the barrierless case, where  $E \approx 0$ , in which case  $k_{\text{IC}}$  will be dominated by diffusion on, and the shape of, the excited-state potential energy surface. A simple model of diffusion on a flat excited surface to symmetrically placed intersections with the ground state was presented by Oster and Nishijima (ON), to model the strong  $\eta$  dependence of the fluorescence of the dye auramine O.<sup>38</sup> The ON model also predicts a linear dependence of  $k_{\text{IC}}$  on  $\eta^{-1}$ . This model also described the isomerization of malachite green observed in *n*-alcohols by Ben-Amotz and Harris.<sup>39</sup> More general models for barrierless isomerization reactions have been described, taking account of the curvature of the excited potential surface, and the fact that the intersection of ground and excited states (“sink”) may not be localized.<sup>40</sup> These models predict more complex forms for the friction dependence. This is consistent with experiment in the sense that a number of experimental observations of a nonlinear dependence of  $k_{\text{IC}}$  on  $\eta^{-1}$  have been reported.<sup>23,41</sup> Unfortunately the parameters required to quantitatively model these results are not usually available. However, from an experimental point of view the empirical formula:

$$k_{\text{IC}} = C/\eta^\alpha \quad (3)$$

where  $C$  is a constant of proportionality has been found to describe a wide range of data, and has a sound theoretical basis in the case of both frequency-dependent friction and other models of reaction dynamics in solution.<sup>42,43</sup> This equation will be employed in the analysis of the data presented below.

### 3. Results and Discussion

#### 3.1. Stationary-State Measurements of $k_{\text{IC}}$ in *n*-Alcohols.

The temperature-dependent fluorescence excitation and emission spectra of **I** in ethanol are shown as a function of temperature in Figure 1. The strong dependence of  $\Phi_f$  on temperature is obvious. On the scale of Figure 1 the emission spectrum only appears above the baseline for  $T < 120$  K, although spectra are resolvable up to at least 293 K, where  $\Phi_f \approx 10^{-4}$ . The

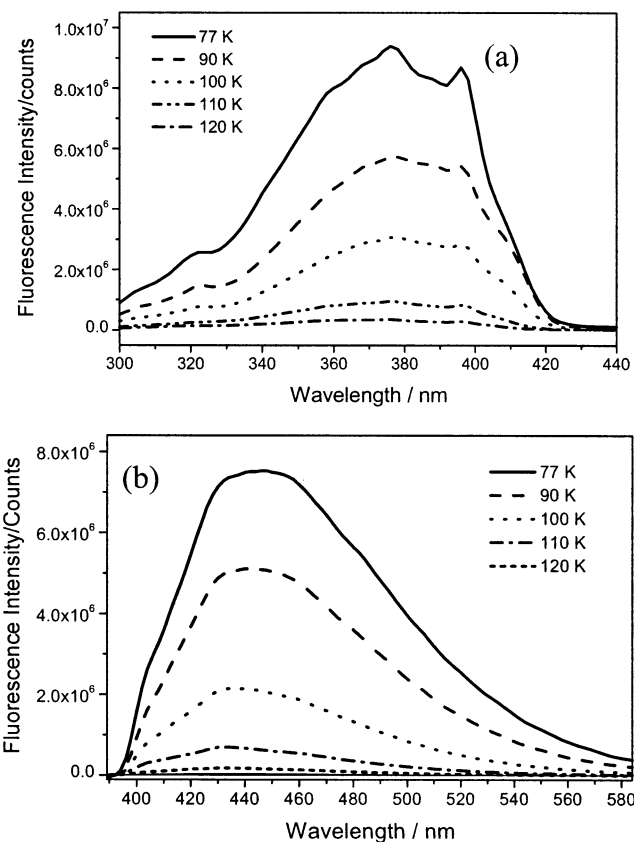


**Figure 1.** Electronic spectra of **I** in ethanol, measured as a function of temperature: (a) excitation and (b) emission spectra.

temperature dependence is so strong that the full set of data may only be observed on a logarithmic scale.<sup>15</sup> It is apparent from Figure 1b that the spectrum does not shift dramatically as  $\Phi_f$  increases. All that is observed in the *n*-alcohol solvents is the appearance of weak vibronic structure at low temperature. The weak dependence of emission and excitation profiles on solvent (data not shown<sup>31,32</sup>) and temperature supports the assumption of a temperature independent  $k_f$ .

In Figure 2  $k_{\text{IC}}$ , calculated according to eq 1, are shown (a) for **I** in four different *n*-alcohols; (b) for **I**, **I**<sup>+</sup>, and **II** in ethanol; and (c) for **I**<sup>+</sup> in four non-*n*-alcohol solvents. The remarkable feature of these data is their uniformity. From the collected data of Figure 2a it is apparent that  $k_{\text{IC}}$  does exhibit a weak but reproducible sensitivity to the physical state of the solvent. There is no obvious change in the exponential temperature dependence of  $k_{\text{IC}}$  as the temperature decreases through the glass transition temperature  $T_g$ . However, in all solvents a moderate increase in the temperature dependence is seen with decreasing temperature through or around the solvent's melting temperature  $T_m$ . Quantitatively, if the data are analyzed according to a simple Arrhenius dependence, at temperatures below  $T_m$  the apparent activation energy is  $(12 \pm 2)$  kJ mol<sup>-1</sup>, while above  $T_m$  it is  $(6 \pm 3)$  kJ mol<sup>-1</sup> (these uncertainties covers all five *n*-alcohol data sets).

The striking feature in Figure 2b is the similar form of the temperature dependence for all three charge forms of **I**, and between **I** and **II**, i.e., the neutral, cationic, and anionic model compounds for GFP and one of its blue-emitting mutants all reveal a common behavior, of a strongly temperature-dependent rate of IC. Since within this series the integrity of the chromophore is maintained, but chromophore charge and H-bond donor and acceptor sites are both modified, it may be concluded that the strong temperature-dependent IC is a property

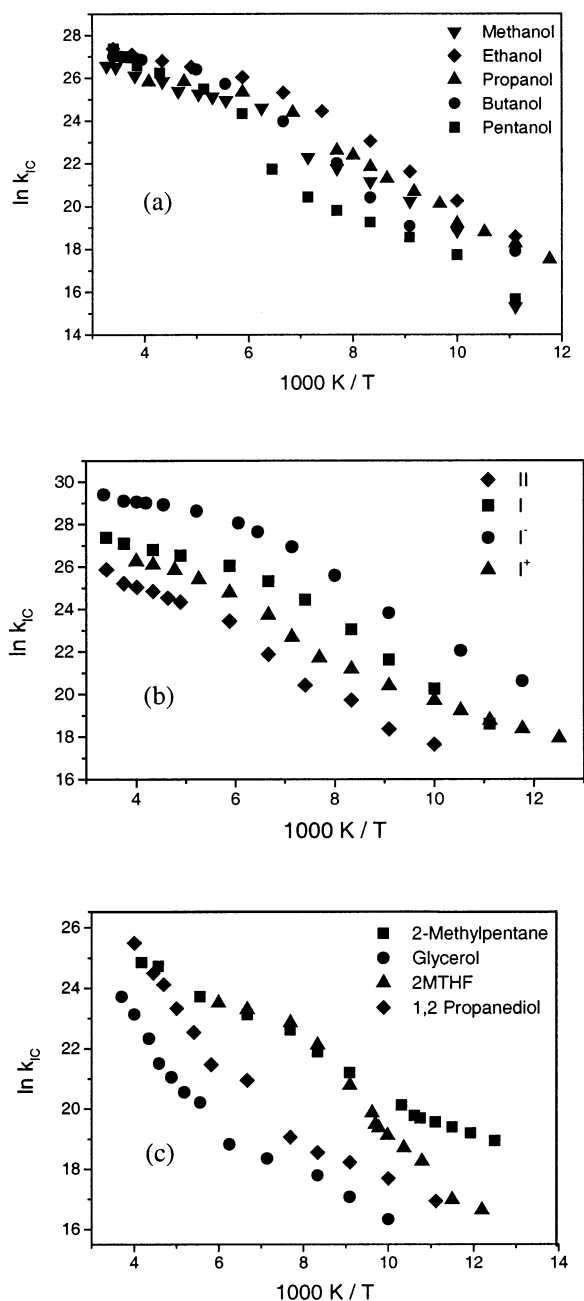


**Figure 2.** Arrhenius plots of  $k_{IC}$  measured for (a) **I** in *n*-alcohols; (b) **I**, its anion, and cation and **II** in ethanol; and (c) **I** in solvents other than *n*-alcohols. For reference, the  $T_g$  values are for methanol 102 K, ethanol 95 K, propanol 100 K, butanol 118 K, 1,2-propanediol 153 K, glycerol 193 K, and 2MTHF 91 K, while  $T_m$  values are for methanol 175 K, ethanol 155 K, propanol 146 K, butanol 183 K, and pentanol 195 K.

of the basic skeleton of the chromophore. It may also be concluded that the suppression of IC is indeed a result of the protein–chromophore interaction, rather than the generation of a chemically modified form of the chromophore in the protein.

The absolute differences between the four data sets in Figure 2b scale approximately with the oscillator strength of the transitions.<sup>32</sup> Since this is related to  $k_f$  (e.g., through the Strickler–Berg relation<sup>44</sup>) it is tempting to assign this dependence to the factor  $k_f$  in eq 1. However a firm conclusion cannot be reached, since the absolute value of  $\Phi_f$  is not known at 77 K, and changes in its value between the different forms of the chromophore will also cause the observed vertical shift of the temperature-dependent curves.<sup>31</sup>

**3.2. Glass Dynamics: A Mechanism for Non-Arrhenius Behavior?** The reproducible appearance of a “knee” in the temperature dependence of  $k_{IC}$  well above  $T_g$  is reminiscent of the observations of Ye et al. for the fluorescence decay time of the triphenyl methane dye malachite green in a range of solvents.<sup>45</sup> It is established that the radiationless relaxation of malachite green occurs through internal conversion promoted by a propeller like rotation of the three phenyl rings.<sup>39</sup> Ye et al. found a knee in the temperature dependence of the excited-state lifetime approximately 30 K above  $T_g$  in *n*-propanol. This was coincident with the critical (or crossover) temperature,  $T_c$ , 30–50 K above  $T_g$ , predicted by the mode-coupling theory of the dynamics of glass-forming liquids.<sup>46</sup> Thus, the non-Arrhenius behavior seen in Figure 2 is the first clear evidence for an effect of the state of the matrix on IC in **I** and **II**. It should be noted that the apparent influence of  $T_c$  on  $k_{IC}$  revealed in Figure 2 is not a simple viscosity effect, since the viscosity of *n*-propanol is very large by 150 K.<sup>47</sup> Rather the effect is a microscopic one, perhaps indicating the breakdown of the hydrodynamic approximation at these high values of  $\eta$ . In some models<sup>48</sup>  $T_c$  is associated with the first appearance of “tight cages” in the liquid, which, in the case of the IC reactions considered here, might possibly act to constrain even small scale intramolecular motion (see below).

Before making a firm assignment of the form of the temperature dependence of IC in **I** and **II** to the influence of glassy dynamics, some significant differences between the present data and those reported for malachite green should be noted. First IC in triphenyl methane dyes has a linear viscosity dependence at elevated temperatures,<sup>39</sup> whereas the dependence for **I** is very weak.<sup>15–17</sup> This does not itself exclude a role for glass dynamics, but does suggest the friction experienced by the coordinates are different in the two cases. Second  $T_c$  is reported in *n*-propanol at 126 K, whereas in Figure 2 the knee is observed at ca. 150 K. Third, Ye et al. reported a strong dependence of excited-state lifetime on temperature above  $T_c$ , which became less marked below  $T_c$ , and still less strong below  $T_g$ . In contrast the 150 K knee corresponds to a transition to a stronger temperature dependence. While the onset of a stronger temperature dependence is consistent with the picture of the onset of strong caging at  $T_c$ ,<sup>48</sup> there may be other explanations for the seemingly temperature (or matrix) dependent value for the isoviscosity activation energy isolated below. Finally, the onset of  $T_c$  is associated with structural relaxation times of the order of 1 ns,<sup>49</sup> whereas the excited-state relaxation time of **I** and **II** at around 150 K is estimated to be <50 ps, on the basis of the excited-state lifetime at 294 K<sup>18</sup> and the measured fluorescence intensity.

**3.3. Stationary-State Measurements of  $k_{IC}$  in Other Media.** The data for **I** in a nonpolar (2 methylpentane, 2MP) and a polar non-H-bonding solvent (2MTHF) (Figure 2c) are broadly consistent with the observations in *n*-alcohols (Figure 2a). This again suggests that the IC reaction is intrinsic to the chromophore structure, rather than a result of a particular solvent–solute interaction. The only significant differences between these data and those in the *n*-alcohols are that the vibronic structure in the non-H-bonding solvents is much better resolved, and the apparent activation energy is in the case of 2MP rather small ( $4 \pm 1$ ) kJ mol<sup>-1</sup>.<sup>32</sup> The only solvents to show qualitatively different behavior to the *n*-alcohols, which form “fragile” glasses,<sup>50</sup> are glycerol (a “strong” glass) and 1,2 propanediol. These solvents have the highest  $T_g$  studied, so  $\Phi_f$  can be observed over a wide temperature range in the glass phase. It is seen that the apparent activation energy decreases for

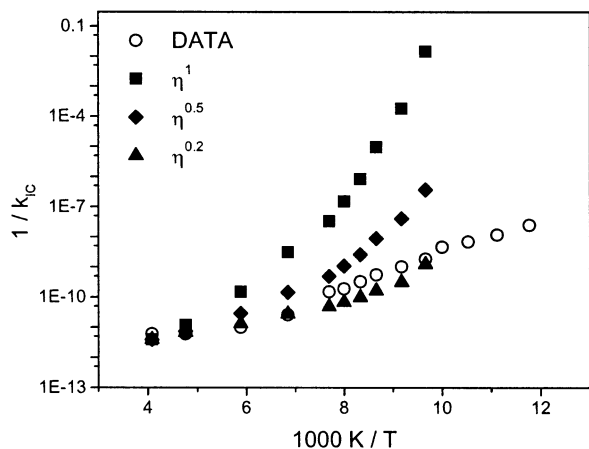


**Figure 3.** Comparison of the temperature dependence of  $\tau_{IC} = 1/k_{IC}$  of **I** in ethanol with the viscosity raised to different fractional powers (cf equation 3).

temperatures below  $T_g$ , which was not seen for **I** or **II** in the *n*-alcohols, but was reported by Ye et al. for malachite green.<sup>45</sup> However it should be noted that the apparent activation energy above  $T_g$  is anomalously high,  $(17 \pm 2)$  kJ mol<sup>-1</sup>, compared to the other H-bonding solvents  $(12 \pm 2)$  kJ mol<sup>-1</sup>; below  $T_g$   $(6 \pm 2)$  kJ mol<sup>-1</sup> is recovered.

The temperature dependence of the quantum yield of **I** has also been studied in a PMMA matrix between 250 and 77 K. The results were similar to those of Figure 2, in that the yield was strongly dependent on temperature, but no large changes in the fluorescence spectral profile were observed. Measurements could not be made at the higher temperatures as an impurity in the PMMA matrix gave a weak emission, which obscured that of **I** for  $T > 250$  K. The impurity emission measured at 295 K was subtracted from all measurements prior to analysis. The Arrhenius plot of the radiationless rate calculated according to eq 1 between 250 and 100 K yields an apparent activation energy of  $(3.8 \pm 1)$  kJ mol<sup>-1</sup>. This is similar to the low value found for the nonpolar solvent 2MP over a wide temperature range, and also similar to the value extracted from the low-temperature isoviscosity analyses described below. This is further evidence for a small intrinsic barrier to IC, at least at low temperatures or in rigid media, and a weak dependence on macroscopic viscosity.

**3.4. Isoviscosity Analysis of Stationary-State  $k_{IC}$ .** One of the important questions to be addressed is whether the temperature dependence of the IC reaction in **I**, revealed in Figure 2, can be regarded as a barrierless process controlled only by medium friction. A barrierless excited-state twisting reaction is predicted for **I** by some theoretical calculations.<sup>10,25</sup> One consequence of this would be to suggest that in GFP the protein matrix suppresses radiationless relaxation by constraining intramolecular motion in the chromophore. Earlier experiments were restricted to 294 K, where solvent viscosities are well-known, but the accessible viscosity range is somewhat limited. As a result it was only possible to conclude that  $k_{IC}$  is a weak function of viscosity,<sup>16–18</sup> in contrast to the behavior of some well-known barrierless isomerization reactions.<sup>39</sup> However, *n*-propanol is one solvent for which the viscosity has been measured over a very wide temperature range, from 293 K down to a few Kelvin above  $T_g$ , encompassing more than 10 decades in viscosity.<sup>47</sup> This makes possible a comparison with experiment over a greatly extended range of viscosity. In Figure 3 the experimental data for **I** in *n*-propanol, extracted according to eq 1 are compared with the predictions of eq 3 (i.e., assuming  $E = 0$ ) for three different values of  $\alpha$ . Note that **I** does not

reach its maximum quantum yield until the temperature falls well below  $T_g$ , where the viscosity is effectively infinite. The constant  $C$  was chosen to normalize the experimental and calculated data at 250 K. As can be seen, these data are consistent with a weak viscosity dependence of the rate of IC. If the IC process is indeed activationless than the entire range of data, down to  $T_g$ , are approximately described by eq 3 with  $\alpha \approx 0.2$ . The implications of such a weak viscosity dependence will be discussed below, after the possibility of an activation barrier to the IC reaction has been considered.

A plausible explanation for the strong temperature dependence of the IC of **I**, which persists even below  $T_g$ , is the existence of a barrier in the coordinate leading to IC. Any such barrier must be small, for the IC to be so efficient, and thus might not have been detected in the MO calculations. In Figure 4a,b the isoviscosity Arrhenius plots are shown for **I**<sup>-</sup> and **II**. The viscosity range here is restricted to low viscosity (1–10 cP) where the hydrodynamic approximation seems to be valid in a number of cases. All data are recorded in *n*-alcohols, to minimize specific solvent effects. The disadvantage of this choice of conditions is that  $\Phi_f$  is small at the relevant temperature, so that solvent background and Raman have to be carefully subtracted.<sup>31</sup> The data in Figures 4a,b are inconclusive, but suggest a small positive activation energy of  $(2 \pm 2)$  kJ mol<sup>-1</sup>. The large uncertainty may be a result of underlying specific solvent effects, for example, on  $E$ ,  $k_f$ , or  $\Phi_f$ ,<sup>77</sup> not accounted for in the analysis.

In an effort to improve the accuracy of the isoviscosity analysis measurements were made at lower temperatures, where  $\Phi_f$  is larger. This however requires the use of the limited range of solvents for which low-temperature viscosities have been determined.<sup>47</sup> In Figure 4c the isoviscosity analysis in the range  $10^4$ – $10^{10}$  cP are presented. Overall the data suggest a positive isoviscosity activation energy of the order of  $(3 \pm 1)$  kJ mol<sup>-1</sup>. Again there is evidence for some specific solvent–solute interactions, which cause the isoviscosity analysis to be less accurate than the Arrhenius plot for a single solvent. A comparison of the isoviscosity data with the data for the individual solvents shows that the apparent (Arrhenius) activation energies are certainly larger than the isoviscosity activation energy.

Taken together the steady-state data suggest that part, but not all, of the temperature dependence of the fluorescence of **I** and **II** can be assigned to IC over a low activation barrier. Interestingly the barrier appears to be greater at lower temperature. It has not proved possible to distinguish whether this corresponds to a real change in the barrier to IC, or to a change in the microscopic friction associated with changes in the solvent dynamics at and below  $T_c$  (to which the model based on the hydrodynamics approximation might not be sensitive).

**3.5. Ultrafast Measurements and Isoviscosity Analysis of  $k_{IC}$  at 293 K.** The steady-state data described above suggest a small activation barrier to IC, which becomes larger at lower temperature. The question of whether the IC reaction is truly barrierless in fluid solvents at 295 K is addressed here by direct measurements of  $k_{IC}$  using ultrafast polarization spectroscopy. Unfortunately, such measurements could not be made at lower temperatures due to strong light scattering from the cryostat obscuring the signal. A typical temperature-dependent data set is shown in Figure 5. Note that the measured ground-state recovery is not well described by a single-exponential function, so the  $k_{IC}$  reported are obtained from the average of the two fastest relaxation times, as described previously.<sup>16</sup> Such non-single-exponential dynamics are predicted by some models of

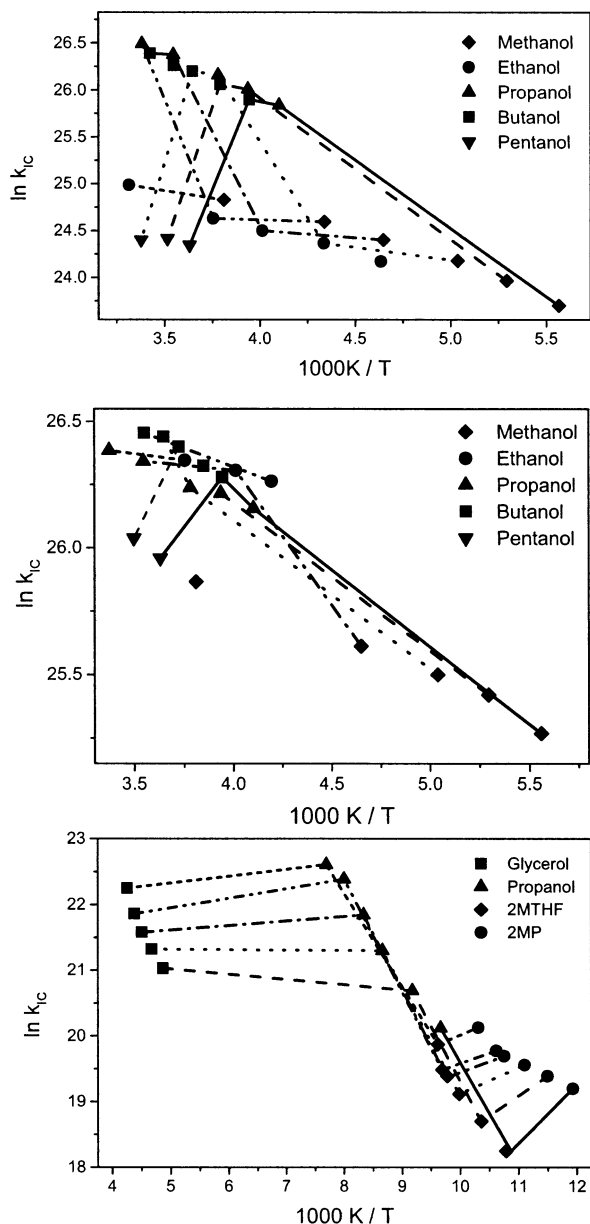


**Figure 4.** Isoviscosity analysis, in which isoviscosities are connected by lines and individual data sets in particular solvents are indicated by symbols. (a)  $\text{II}$  in *n*-alcohols where the viscosities are 10 cP (solid), 7 cP (dash), 5 cP (dot), 3 cP (dash-dot), 2 cP (dash-dot-dot), and 1 cP (short dash). (b) The anionic form of  $\text{I}$  in *n*-alcohols, where the lines represent the same viscosities as those in (a). (c)  $\text{I}$  in a range of solvents  $10^{10}$  cP (solid),  $2 \times 10^8$  cP (dash),  $10^7$  cP (dot),  $10^6$  cP (dash-dot),  $2 \times 10^5$  cP (dash-dot-dot), and  $4 \times 10^4$  cP (short dash).

barrierless isomerization reactions.<sup>40</sup> The minor long-lived component in the recovery is due to solute orientational relaxation.<sup>16</sup>

In Figure 6 the  $k_{IC}$  data measured in a range of different basic alcohol solvents at various temperatures are analyzed assuming a barrierless reaction (i.e., eq 3) for both the neutral and the anionic forms of  $\text{I}$ . These data reveal a weak dependence on viscosity (with a wide range of scatter between different solvent). Fitting the data to a linear function yields the exponent in eq 3,  $\alpha = 0.25 \pm 0.06$ . This is comparable to the value extracted from analyzing the steady-state data for  $\text{I}^-$  measured over an extended temperature range in *n*-propanol (Figure 3).

In Figure 7 the isoviscosity analysis for the  $k_{IC}$  of  $\text{I}^-$  at temperatures above 295 K is presented. A thermally activated radiationless process is seen in each individual solvent (e.g.,

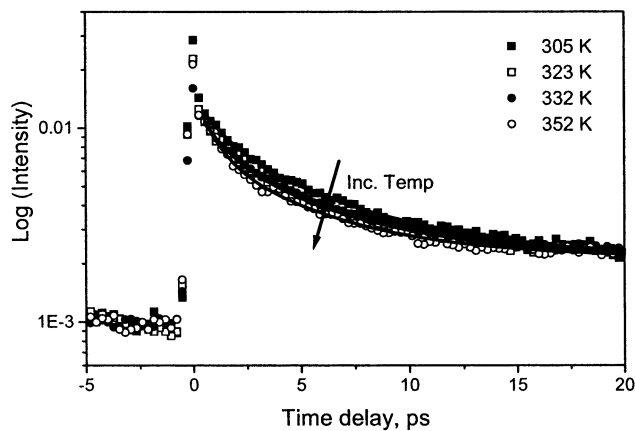


**Figure 5.** Ultrafast ground-state recovery dynamics for the anion of  $\text{I}$  in *n*-butanol as a function of temperature.

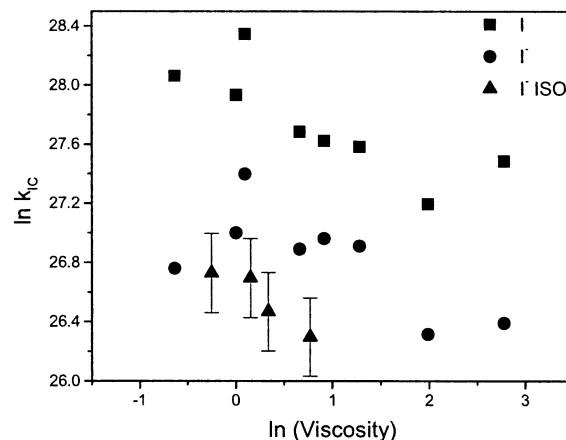


**Figure 6.** A plot of  $k_{IC}$  obtained from the ultrafast recovery dynamics plotted as a function of the medium viscosity. Data are shown for  $\text{I}$  and its anion in a range of solvents, and for the anion measured in *n*-alcohols, in which the temperature was adjusted to yield the four viscosities. For the latter the error bars are adjusted to cover the range of the measurements. The error bars will be similar for all measurements.

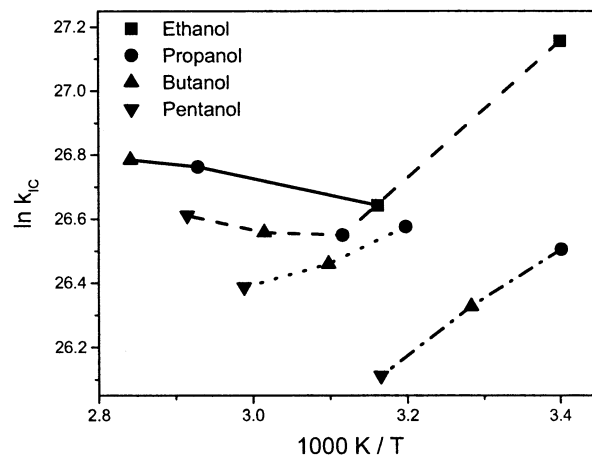


**Figure 7.** Isoviscosity analysis of the ultrafast transient data for the anion of  $\text{I}$  in the solvents indicated. The viscosities are 0.78 cP (solid), 1.16 cP (dash), 1.4 cP (dot), and 2.16 cP (dash-dot).

Figure 5). However, the isoviscosity analysis reveals negative isoviscosity activation energies at three out of the four viscosities studied, albeit with a very large mean error. A negative activation energy is an unexpected but not unprecedented result.<sup>39</sup> For example, it may arise from specific solvent effects on the barrier height, which are not accounted for in the

isoviscosity analysis. Alternatively a strongly asymmetric ground-state potential energy surface may also lead to a negative apparent activation energy. Whatever the reason for this behavior, the fact that the more precise ultrafast measurements fail to detect an activation barrier at these higher temperatures, while the steady-state analysis detects a small barrier at reduced temperature, is taken to indicate an essentially barrierless process for  $T > 295$  K. Thus IC in **I**<sup>-</sup> at  $T > 295$  K is a barrierless process with a very weak viscosity dependence. The same conclusion may reasonably be drawn for the neutral and cation of **I** and for **II**, based on their similar temperature dependent behaviors (Figure 2).

**3.6. The Nature of the Coordinate Promoting IC.** The results above suggest further details on the nature of the coordinate leading to ultrafast IC. The similarity of the behavior for **I**, its ions, and **II** requires the coordinate to be very similar in all these forms. This suggests the involvement of the bridging single and double bonds, which are common to all structures. This is in accord with a number of theoretical calculations, where near barrierless rotation about this bond in the excited state was reported to causes close approach of ground and excited states, through strong destabilization of the ground state.<sup>10,25</sup> The very weak viscosity dependence observed suggests either that this coordinate does not experience strong friction or that macroscopic viscosity is a poor measure of microscopic friction for this coordinate. The failure of the hydrodynamic approximation for IC in **I** and **II** is not consistent with rotation about either the double or the single bridging bond alone. These would require rotation of either the phenol/benzene ring or the substituted heteroaromatic ring. There is adequate evidence that for moderate viscosities this kind of barrierless internal rotation should occur under hydrodynamic or near hydrodynamic conditions. Some examples include the following: the rotation of the entire molecule **I**;<sup>16,17</sup> the diffusive reorientation of substituted benzene molecules;<sup>34</sup> the intermolecular rotation of phenyl groups in triphenylmethane dyes,<sup>39</sup> diphenylbutadiene,<sup>37</sup> and auramine.<sup>38</sup>

A second potential coordinate for IC in **I** and **II**, which involves the bridging single and double bonds, as required, is a concerted rotation of both bonds, sometimes referred to as the "hula twist" (HT). It is easy to see that this is a volume-conserving coordinate compared to rotation about either bond alone. Indeed, the HT mechanism was originally proposed as a volume-conserving coordinate for isomerization in the confined retinal polyene of rhodopsin.<sup>51</sup> Since the HT coordinate leads to the displacement of only a small solvent volume, it is consistent with the observation of a weak viscosity dependence.

There has been some recent interest in the HT mechanism, as it explains some anomalous (from the point of view of a single-bond rotation mechanism) polyene photoisomerization data measured in the solid phase.<sup>26,27</sup> That the HT mechanism operates in the solid phase is also consistent with the observation that the  $\Phi_f$  of **I** and **II** continues to increase below  $T_g$ . However, it should be noted that if the intramolecular motion required for IC is small tunneling may also operate at low temperature.<sup>52</sup> Most of the discussion of the HT mechanism has assumed that it is a process with a high activation barrier, which becomes significant only when the conventional, solvent displacing, one bond rotation channel is blocked by medium friction.<sup>27</sup> In contrast, in the calculation of Weber and co-workers for **I** and **I**<sup>-</sup> the HT channel was found to be barrierless in the neutral, and to have a significant barrier (40 kJ mol<sup>-1</sup>) only for the anion.<sup>10</sup> Importantly for both **I** and **I**<sup>-</sup>, ground and excited states were seen to approach closely during the HT. Thus the HT

mechanism is consistent with the observed viscosity, charge, and H-bonding state independence of IC in **I** and **II**. However, the calculations on the HT mechanism are inconsistent with the observation of similar and small (or negligible) activation barriers for **I** and **I**<sup>-</sup>. This latter result suggests that (a) more accurate calculation of the HT mechanism as a function of the torsional angle are desirable and/or (b) that the volume-conserving intramolecular motion leading to IC may be more complex than can be represented by a single coordinate, such as HT.

## Conclusion

A detailed study of the temperature and viscosity dependence of the radiationless decay of **I**, its anion, its cation, and **II** has been presented. For all four forms  $k_{IC}$  exhibits a strong dependence on temperature. This temperature dependence does not have a simple Arrhenius form. This may indicate a sensitivity of  $k_{IC}$  to the transition to glassy dynamics at the critical temperature, some 30–70 K above  $T_g$ , predicted by mode-coupling theory. In fragile glasses (the *n*-alcohol solvents)  $k_{IC}$  appears insensitive to the glass transition temperature itself, though in some other solvents a weaker  $T$  dependence is seen below  $T_g$ .

The temperature and viscosity dependence have been separated in an isoviscosity analysis. The IC is found to be barrierless at 295 K, but there is evidence for a small barrier at low temperature, which becomes larger with decreasing temperature. It was proposed that this reflects the influence of glassy dynamics, not accounted for in an isoviscosity analysis, rather than the formation of a true barrier in the coordinate leading to IC.

The present data allow us to quantify our earlier report of a weak viscosity dependence of  $k_{IC}$ . Specifically the exponent  $\alpha$  in eq 3 takes a value of  $0.25 \pm 0.06$ . This suggests that IC is promoted by a coordinate which is only weakly coupled to medium viscosity. One possibility is the volume-conserving "hula twist", which involves the concerted rotation of both of the bridging bonds. Conclusive support for this hypothesis requires more detailed quantum chemical calculations on **I** and **II**. Any further conclusion on the important question of how the protein suppresses IC requires such detailed calculations to be made in the protein matrix.

**Acknowledgment.** The authors are grateful to BBSRC and EPSRC for financial support for this research. N.M.W. thanks EPSRC for a studentship. S.R.M. is grateful to Dr Peter Schellenberg for a preprint of his work.

## References and Notes

- (1) Tsien, R. Y. *Annu. Rev. Biochem.* **1998**, *67*, 509.
- (2) Prendegast, F. G. *Methods Cell Biol.* **1999**, *58*, 1.
- (3) Shimomura, O. *FEBS Lett.* **1979**, *104*, 220.
- (4) Cody, C. W.; Prasher, D. C.; Westler, W. M.; Prendegast, F. G.; Ward, W. W. *Biochemistry* **1993**, *32*, 1212.
- (5) Niwa, H.; Ionuye, S.; Horano, T.; Matsuno, T.; Kojima, S.; Kubota, M.; Ohashi, M.; Tsuji, F. I. *Proc. Natl. Acad. Sci. U. S. A.* **1996**, *93*, 13617.
- (6) Chattoraj, M.; King, B. A.; Bublit, G. U.; Boxer, S. G. *Proc. Natl. Acad. Sci. U. S. A.* **1996**, *93*, 8362.
- (7) Lossau, H.; Kummer, A. D.; Heinecke, R.; Pollinger-Dammer, F.; Kompa, K.; Bieser, G.; Jonson, T.; Silva, C. M.; Yang, M. M.; Youvan, D. C.; Michel-Beyerle, M. E. *Chem. Phys.* **1996**, *213*, 1.
- (8) Kojima, S.; Ohkawa, H.; Hirano, T.; Maki, S.; Niwa, H.; Ohashi, M.; Inouye, S.; Tsuji, F. I. *Tetrahedron Lett.* **1998**, *39*, 5239.
- (9) Kummer, A. D.; Wiehler, J.; Rehner, H.; Kompa, K.; Steipe, B. and Michel-Beyerle, M. E. *J. Phys. Chem. B* **2000**, *104*, 4791.
- (10) Weber, W.; Helms, V.; McCammon, J. A.; Langhoff, P. W. *Proc. Natl. Acad. Sci. U. S. A.* **1999**, *96*, 6177.
- (11) Voityuk, A. A.; Michel-Beyerle, M.-E.; Rösch, N. *Chem. Phys.* **1998**, *231*, 13.

- (12) Voityuk, A. A.; Kummer, A. D.; Michel-Beyerle, M.-E.; Rösch, N. *Chem. Phys.* **2001**, *269*, 83.
- (13) Helms, V.; Winstead, C.; Langhoff, P. W. *J. Mol. Struct. (Theochem)* **2000**, *506*, 179.
- (14) El Yazal, J.; Prendegast, F. G.; Shaw, D. E.; Pang, Y.-P. *J. Am. Chem. Soc.* **2000**, *122*, 11411.
- (15) Webber, N. M.; Litvinenko, K. L.; Meech, S. R. *J. Phys. Chem. B* **2001**, *105*, 8036.
- (16) Litvinenko, K. L.; Webber, N. M.; Meech, S. R. *Chem. Phys. Lett.* **2001**, *346*, 47.
- (17) Litvinenko, K. L.; Webber, N. M.; Meech, S. R. *Bull. Chem. Soc. Jpn.* **2002**, *75*, 1065.
- (18) Mandal, D.; Tahara, T.; Webber, N. M.; Meech, S. R. *Chem. Phys. Lett.* **2002**, *358*, 495.
- (19) Kummer, A. D.; Kompa, C.; Niwa, H.; Hirano, T.; Kojima, S.; Michel-Beyerle, M.-E. *J. Phys. Chem. B* **2002**, *106*, 7554.
- (20) Nielsen, S. B.; Lapierre, A.; Andersen, J. U.; Pedersen, U. V.; Tomita, S.; Anderson, L. H. *Phys. Rev. Lett.* **2001**, *87*, 228102.
- (21) Schellenberg, P.; Johnson, E.; Esposito, A. P.; Reid, P. J.; Parson, W. W. *J. Phys. Chem. B* **2001**, *105*, 5316.
- (22) Stübner, M.; Schellenberg, P. *J. Phys. Chem. A* **2003**, *107*, 1246.
- (23) Velsko, S. P.; Waldeck, D. H.; Fleming, G. R. *J. Chem. Phys.* **1983**, *78*, 249.
- (24) Sun, Y.-P.; Saltiel, J. *J. Phys. Chem.* **1989**, *93*, 8310.
- (25) Voityuk, A. A.; Michel-Beyerle, M.-E.; Rösch, N. *Chem. Phys. Lett.* **1998**, *296*, 269.
- (26) Liu, R. S. H. *Acc. Chem. Res.* **2001**, *34*, 555.
- (27) Liu, R. S. H.; Hammond, G. S. *Proc. Natl. Acad. Sci. U. S. A.* **2000**, *97*, 11153.
- (28) Chalfie, M.; Kain, S. R., Eds. *Green Fluorescent Protein: Properties, Applications, Protocols*; Wiley: New York, 1998.
- (29) Alavi, D. S.; Hartman, R. S.; Waldeck, D. H. *J. Chem. Phys.* **1990**, *92*, 4055.
- (30) Cross, A. J.; Waldeck, D. H.; Fleming, G. R. *J. Chem. Phys.* **1983**, *78*, 6455.
- (31) Webber, N. M., Ph.D. Thesis, University of East Anglia, Norwich, U. K., 2002.
- (32) Webber, N. M.; Meech, S. R. In preparation.
- (33) Perozzo, M. A.; Ward, K. B.; Thomson, R. B.; Ward, W. W. *J. Biol. Chem.* **1988**, *263*, 7716.
- (34) Smith, N. A.; Meech, S. R. *J. Phys. Chem. A* **2000**, *104*, 4223.
- (35) Bauer, D. L.; Brauman, J. I.; Pecora, R. *J. Am. Chem. Soc.* **1974**, *96*, 6840.
- (36) Kramers, H. A. *Physica* **1940**, *7*, 284.
- (37) Keery, K. M.; Fleming, G. R. *Chem. Phys. Lett.* **1982**, *93*, 322.
- (38) Oster, G.; Nishijima, Y. *J. Am. Chem. Soc.* **1956**, *78*, 1581.
- (39) Ben-Amotz, D.; Harris, C. B. *J. Chem. Phys.* **1987**, *86*, 4856.
- (40) Bagchi, B.; Fleming, G. R.; Oxtoby, D. W. *J. Chem. Phys.* **1983**, *78*, 7375.
- (41) Park, N. S.; Waldeck, D. H. *J. Phys. Chem.* **1990**, *94*, 662.
- (42) Bagchi, B.; Oxtoby, D. W. *J. Chem. Phys.* **1983**, *78*, 2735.
- (43) Sumi, H. In *Electron Transfer: From Isolated Molecules to Biomolecules*; Jortner, J., Bixon, M., Eds.; Advances in Chemical Physics 107; Wiley and Sons: New York, 1999; Part 2, p 601.
- (44) Strickler, S. G.; Berg, R. A. *J. Chem. Phys.* **1962**, *37*, 814.
- (45) Ye, J. Y.; Hattori, T.; Inouye, H.; Ueta, H.; Nakatsuka, H.; Maruyama, Y.; Ishikawa, M. *Phys. Rev. B* **1996**, *53*, 8349.
- (46) Götze, W.; Sjögren, L. *Rep. Prog. Phys.* **1992**, *55*, 241.
- (47) Ling, A. C.; Willard, J. E. *J. Phys. Chem.* **1968**, *72*, 1918.
- (48) Tanaka, H. *J. Chem. Phys.* **1996**, *105*, 9375.
- (49) Sokolov, A. P. *J. Non-Cryst. Solids* **1998**, *235-7*, 190.
- (50) Angell, C. A. *J. Phys. Chem. Solids* **1988**, *49*, 863.
- (51) Liu, R. S. H.; Asato, A. E. *Proc. Natl. Acad. Sci. U. S. A.* **1985**, *82*, 259.
- (52) Engelman, R.; Jortner, J. *Mol. Phys.* **1970**, *18*, 145.